

Inelasticity distribution and relationship between e^+e^- and pp hadron-production mechanisms

K. Kadija* and M. Martinis

Ruder Bošković Institute, P.O.B. 1016, 41001 Zagreb, Croatia

(Received 20 January 1992; revised manuscript received 3 March 1993)

The inelasticity distribution is used to relate the hadron-production data in e^+e^- annihilation to the corresponding data in pp collisions. If e^+e^- annihilation data are used as input, the hadron multiplicity distributions $P_n(s)$, the average multiplicities $\langle n'(s) \rangle$, the normalized moments $C'_q(s)$, the energy dependence of the average transverse momentum $\langle p_T(s) \rangle$, the height of the central plateau $h(s)$, and the strength of the forward-backward multiplicity correlations $b(s)$ are qualitatively reproduced over the range of energies from those reached at the CERN ISR to $\sqrt{s} = 900, 1800, \text{ and } 10^4 \text{ GeV}$ in pp collisions. The discrepancies observed between predicted and experimental values of $C'_q(s)$, $q \geq 4$, and $h(s)_{pp}$ are indicated and commented upon. Other possible tests of the e^+e^-pp universality are briefly mentioned.

PACS number(s): 13.85.Hd, 12.40.Ee, 13.65.+i

I. INTRODUCTION

The idea of a universal hadronization mechanism is not new. It is based on the observation [1,2] that the characteristics of low- p_T hadron jets associated with leading protons in pp collisions are similar to hadron jets observed in high-energy e^+e^- annihilation provided that comparisons are made at the same proper energy for hadron production.

In pp collisions, the proper energy for hadron production is the energy left behind by the two leading protons. It is defined as the invariant mass squared of the produced hadron system [2]:

$$W^2 = (p_1 - p_{1 \text{ leading}} + p_2 - p_{2 \text{ leading}})^2 = (p_{1 \text{ had}} + p_{2 \text{ had}})^2, \quad (1.1)$$

where p_1, p_2 denote the four-vectors of the initial protons and $p_{1 \text{ leading}}, p_{2 \text{ leading}}$ are the same outgoing leading protons. If the transverse momenta of the leading protons are negligible, then

$$W \approx E_{1 \text{ had}} + E_{2 \text{ had}}.$$

In the special case of symmetric events where $E_{1 \text{ had}} = E_{2 \text{ had}}$ and $\mathbf{p}_{1 \text{ had}} = -\mathbf{p}_{2 \text{ had}}$ we have

$$W = 2E_{\text{had}} = (\sqrt{s})_{pp} - 2E_{\text{leading}}. \quad (1.2)$$

In e^+e^- annihilation into hadrons, the proper energy for hadron production coincides with the total c.m. energy of the beam:

$$(\sqrt{s})_{e^+e^-} = 2E_{\text{beam}} = W. \quad (1.3)$$

A remarkable similarity between pp collisions and e^+e^- annihilation has been found in the inclusive momentum distribution and the mean multiplicity of

charged particles up to the highest energies reached at the DESY e^+e^- collider PETRA and CERN Intersecting Storage Rings (ISR) [3] if the data are analyzed at the same equivalent energy:

$$(\sqrt{s})_{pp} - 2E_{\text{leading}} = W = (\sqrt{s})_{e^+e^-}. \quad (1.4)$$

A long-standing problem in multiparticle phenomenology is whether there is a relation between hadron production characteristics in pp and e^+e^- collisions. In the absence of a firm theory on pp collisions, various conflicting answers have been given to this question [4–9]. Although the problem is an old one, currently popular models, such as FRITIOF from the Lund group [10], still describe soft processes as a superposition of e^+e^- and deep inelastic processes. However, there are limits to such an analogy [7,9], in particular concerning the p_T structure of both processes at higher energies, $\sqrt{s} > 100 \text{ GeV}$. With increasing energy, the violation of the Koba-Nielsen-Olesen (KNO) scaling [11] in pp and/or $\bar{p}p$ collisions is observed in the CERN ISR data [12] and in the CERN Super Proton Synchrotron (SPS) collider data [13,14]. At the same time, the approximate KNO scaling in e^+e^- annihilation is observed in the energy interval from $(\sqrt{s})_{e^+e^-} \approx 20$ to 91 GeV [15–17].

This paper may be considered as an additional contribution to the above discussion of a possible link between e^+e^- and pp interactions extended to higher incoming energies for hadron production. The link between e^+e^- and pp collisions is provided by appropriate smearing of the e^+e^- data over inelasticity [18]. Our discussion will be restricted to the prediction of the energy dependence of the following physical quantities: the charged multiplicity distributions $P_n(s)$, the average charged multiplicity $\langle n(s) \rangle$, the multiplicity dispersion $D(s)$, the normalized moments $C'_q(s)$, the average transverse momentum $\langle p_T(s) \rangle$, the height of the central plateau, and the strength of forward-backward charged-particle multiplicity correlations in pp collisions.

The outline of the paper is as follows. In Sec. II we define the inelasticity distribution and establish its con-

*Also at the Max-Planck-Institut, München, Germany.

nection with the universality hypothesis. In Sec. III we list some of the known experimental data on e^+e^- annihilation in the energy region from $\sqrt{s} \approx 20$ to 91 GeV. These data are then used in Sec. IV as input to predict the behavior of the hadron system produced in pp collisions up to $(\sqrt{s})_{pp} \approx 10^4$ GeV. In Sec. V we compare our model predictions with pp collision data. In Sec. VI we add a few concluding critical remarks concerning the extension of the model to still higher energies.

II. INELASTICITY DISTRIBUTION

In their analysis of the data on hadron production, Basile *et al.* [1] emphasized the importance of the leading-particle effect and the use of the energy variable E_{had} for hadron production. The inelasticity K of the collision is related to E_{had} by

$$2E_{\text{had}} = K\sqrt{s} . \quad (2.1)$$

It describes the fraction of incoming c.m. energy \sqrt{s} that fragments into hadrons in the central region. Since E_{had} varies at fixed \sqrt{s} from event to event, it is necessary to introduce a probability distribution function $\chi(K,s)$ of the inelasticity variable K with the normalization

$$\int_0^1 \chi(K,s) dK = 1 . \quad (2.2)$$

All the ‘‘intrinsic’’ physical observables depending on K are now to be smeared up over $\chi(K,s)$.

As pointed out by Fowler *et al.* [18], the dependence of $\chi(K,s)$ on s is essential for a satisfactory account of the data. No completely satisfactory theoretical derivation of $\chi(K,s)$ exists [18,19]. Experimental information on $\chi(K,s)$ is, however, available only for $(\sqrt{s})_{pp} = 16.5$ GeV [20] with a maximum at $K \sim 0.5$. The mean inelasticity $\langle K \rangle$, defined as

$$\langle K \rangle = \int_0^1 K \chi(K,s) dK , \quad (2.3)$$

is approximately constant up to ISR energies ($\langle K \rangle \sim 0.5$).

If $P(n|K)$ denotes the ‘‘intrinsic’’ conditional probability of observing n charged particles provided that the inelasticity of an event is K , then the experimentally measured charged-particle multiplicity distribution $P_n(s)$ is obtained as a convolution:

$$P_n(s) = \int_0^1 dK \chi(K,s) P(n|K) . \quad (2.4)$$

The information on $P(n|K)$ and its dependence on K may, in principle, be obtained from data [15] using the relation (2.4) and the information on $\chi(K,s)$. We shall, however, follow another approach suggested by the finding of Basile *et al.* [1]. We assume that, in the first approximation, $P(n|K)$ is given by the normalized multiplicity distribution for e^+e^- annihilation over a range of energies where $(\sqrt{s})_{e^+e^-} = W = K(\sqrt{s})_{pp}$. In this approach, the starting relation is

$$P_n(s)_{pp} = \int_{K_{\min}}^1 dK \chi(K,s) P_n(K\sqrt{s})_{e^+e^-} , \quad (2.5)$$

where $K_{\min} = 2m_\pi/\sqrt{s}$ is due to the threshold energy for

the two-pion final state in e^+e^- annihilation.

A simple relationship between $P_n(s)_{pp}$ and $P_n(K\sqrt{s})_{e^+e^-}$ [by Eq. (2.5)] requires the knowledge of the function $\chi(K,s)$. The energy dependence of $\chi(K,s)$ or of its moments

$$\langle K^r \rangle = \int_0^1 dK K^r \chi(K,s) , \quad r = 1, 2, \dots , \quad (2.6)$$

is related to the problem of violation of the Feynman scaling in the fragmentation region of the leading particles. The available experimental data related to the energy dependence of the leading-proton distribution are inconclusive. The leading-proton spectrum was studied experimentally only at ISR energies [21], but not at CERN or Fermilab $p\bar{p}$ colliders. As a consequence, very little is known about the energy dependence of inelasticity. Several authors have assumed that the average inelasticity is a decreasing function of energy [18,19,22–24] and others have assumed that inelasticity is an increasing function of energy [25]. We find that the arguments offered in Refs. [24,26] that the inelasticity $\langle K \rangle$ is a decreasing function of energy are more convincing and solid.

The first attempts to construct $\chi(K,s)$ with this property were merely a simple parametrization. Following Fowler *et al.* [19], we shall take $\chi(K,s)$ in the form of a β distribution:

$$\begin{aligned} \chi(K,s) &= K^{a-1} (1-K)^{b-1} / B(a,b) , \\ B(a,b) &= \Gamma(a)\Gamma(b) / \Gamma(a+b) , \end{aligned} \quad (2.7)$$

with

$$\langle K \rangle = a/(a+b) \quad \text{and} \quad \langle K(1-K) \rangle / D^2(K) = a+b .$$

The s dependence of $\chi(K,s)$ is contained in the parameters a and b , which are determined by measuring $\langle K \rangle$ and $D^2(K) = \langle K^2 \rangle - \langle K \rangle^2$, respectively.

III. INPUT INFORMATION ON e^+e^-

The data on e^+e^- annihilation are now available from $(\sqrt{s})_{e^+e^-} \approx 20$ up to 91 GeV [16,17].

The charged multiplicity distribution. The charged multiplicity distribution of hadrons for this limited range of energy is consistent with the approximate KNO scaling [17]. The KNO-scaling function that provides a good continuous representation of the data is [4,6,27]

$$\begin{aligned} \langle n(W) \rangle_{e^+e^-} &= P_n(W)_{e^+e^-} \\ &= \psi_{e^+e^-}(z) \\ &= 4(9\pi/16)^2 z^3 \exp[-(9\pi/16)z^2] , \end{aligned} \quad (3.1)$$

where $z = n / \langle n(W) \rangle_{e^+e^-}$ and $\psi_{e^+e^-}(z)$ is normalized as

$$\int dz \psi_{e^+e^-}(z) = \int dz z \psi_{e^+e^-}(z) = 2 ,$$

with

$$W = K\sqrt{s} .$$

Note that $n \equiv n_{\text{ch}} = 2n_-$ for e^+e^- collisions.

The data may also be fitted by the scaling form of the negative-binomial (NB) distribution [17].

The average charged multiplicity. Various parametrizations have been proposed [17] for the average charged multiplicity of hadrons in e^+e^- annihilation. We shall use the power-law dependence on the incoming c.m. energy $W = (\sqrt{s})_{e^+e^-}$:

$$\langle n(W) \rangle_{e^+e^-} = 2.20 W^{1/2}. \quad (3.2)$$

Later on we shall discuss effects that the other parametrizations may have on the derived pp results. The new data from the CERN e^+e^- collider LEP seem to indicate that it is possible to exclude the power-law dependence [17], which is known to follow from various statistical [28] and branching models [29].

The normalized moments C_q . The KNO scaling implies an energy independence of the normalized moments C_q . Data [17] show no indication of an energy variation of C_2 to C_5 for $(\sqrt{s})_{e^+e^-}$ from 20 to 91 GeV. Using (3.1) we find that

$$C_q(e^+e^-) = \left(\frac{4}{3}\right)^q \pi^{-q/2} \Gamma(q/2 + 2). \quad (3.3)$$

From this equation we calculate the dispersion $D = (C_2 - 1)^{1/2} \langle n \rangle$ as

$$D_{e^+e^-}(W) = (32/9\pi - 1)^{1/2} \langle n(W) \rangle_{e^+e^-}. \quad (3.4)$$

The average transverse momentum. The average transverse momentum $\langle p_t(W) \rangle_{e^+e^-}$ of charged hadrons in e^+e^- annihilation is experimentally almost constant with respect to the thrust axis for energies up to $W \simeq 30$ [30]. We parametrize its dependence on W by

$$\langle p_t(W) \rangle_{e^+e^-} = \alpha W + \beta, \quad (3.5)$$

with

$$\alpha = 4.2 \times 10^{-4} / c, \quad \beta = 0.356 \text{ GeV} / c,$$

and assume that it is valid up to $W = 91$ GeV.

The height of the central plateau. The available data for the e^+e^- cross section

$$\left. \frac{1}{\sigma} \frac{d\sigma}{dy} \right|_{y=0} = h(W)$$

at $y = 0$ [16] show that $h(W)$ rises with W , and the trend is well parametrized by

$$h(W) = h_0 + h_1 \ln W, \quad (3.6)$$

with $h_0 = 2.67$ and $h_1 = 0.40$.

Forward-backward multiplicity correlations. The data from $\sqrt{s} = 14$ to 91 GeV [16,17] show weak positive and

approximately energy-independent forward- (F) backward (B) multiplicity correlations. They are fairly well parametrized by a linear function

$$\langle n_F(n_B) \rangle = a + b n_B, \quad (3.7)$$

where b is approximately ~ 0.1 and measures the correlation strength. The observed slight variation of b in the range from $s = 14$ to 91 GeV is taken into account by

$$b = 0.027 \ln \sqrt{s}. \quad (3.8)$$

The approximate KNO scaling in the variable $n = n_F + n_B$ suggests that the probability distribution $P(n_F, n_B | W)$ with respect to forward and backward multiplicities n_F and n_B is a product of two distributions [31,32]:

$$P(n_F, n_B | W) = P_n(W) f_n(\Delta), \quad \Delta = n_F - n_B. \quad (3.9)$$

The distribution $P_n(W)$ is assumed to follow the KNO-scaling rule and is here given by (3.1). It is also required that the distribution $f_n(\Delta)$ at fixed n should be even in the variable Δ , peak at $\Delta = 0$ and have the property

$$\langle \Delta^2 \rangle_n \sim k n \quad \text{if } n \text{ is large}. \quad (3.10)$$

Here k is a parameter between 1 and 2, probably slightly energy dependent.

A simple choice of $f_n(\Delta)$ having these properties is

$$f_n(\Delta) = (\text{norm const}) \times \exp(-\Delta^2/2kn). \quad (3.11)$$

Note that $\Delta = \text{even} = -n, -n+2, \dots, n$. The summations over n_B and n_F are performed using the replacement

$$\sum_{n_F, n_B} \rightarrow \frac{1}{2} \int_0^\infty dn \int_{-n}^n d\Delta.$$

Using (3.1) and (3.4) in (3.9) and (3.10) it is easy to show that, in the large- n limit, the correlation strength b is

$$\begin{aligned} b &= [D^2(n) - k \langle n \rangle] / [D^2(n) + k \langle n \rangle] \\ &= [0.132 \langle n(W) \rangle - k] / [0.132 \langle n(W) \rangle + k]. \end{aligned} \quad (3.12)$$

A reasonable fit to the e^+e^- data is achieved with $k \lesssim 2$. Note that in the case $k = 2$ the correlation parameter b becomes positive only if $W > 30$ GeV.

IV. PREDICTIONS FOR pp COLLISIONS

The charged multiplicity distribution. Using Eqs. (2.5)–(2.7) and Eq. (3.1) we calculate the multiplicity distribution in pp collisions. Taking $K_{\min} \approx 0$, we find that

$$\langle n'(s) \rangle_{pp} P_n(s)_{pp} = 4(9\pi/16)z'^3 \langle K^{1/2} \rangle^3 \exp[-(9\pi/16)z'^2 \langle K^{1/2} \rangle^2] \langle K^{1/2} \rangle \frac{\Gamma(a+b)}{\Gamma(a)} U(b, 3-a, (9\pi/16)z'^2 \langle K^{1/2} \rangle^2), \quad (4.1)$$

where

$$\langle K^{1/2} \rangle = \frac{B(a + \frac{1}{2}, b)}{B(a, b)}, \quad z' = n / \langle n'(s) \rangle_{pp}, \quad (4.2)$$

and $U(b, 3-a, \dots)$ is Kummar's function [33]. The prime on $\langle n'(s) \rangle_{pp}$ indicates that the contributions from leading particles are missing. The correct expression for the average charged hadron multiplicity in pp collisions should be

$$\langle n(s) \rangle_{pp} = \langle n'(s) \rangle_{pp} + n_0, \quad (4.3)$$

with n_0 being the measure of the average number of charged leading particles. For leading protons we shall use $n_0 = 2$ [29].

Since, in our approach, $\langle K^{1/2} \rangle$ is a decreasing function of \sqrt{s} , the multiplicity distributions given by (4.1) become broader with increasing \sqrt{s} ; i.e., they have a larger high-multiplicity tail ($z' > 1$) predicting breaking of the KNO scaling in pp collisions.

The average charged multiplicities $\langle n'(s) \rangle_{pp}$. The average charged multiplicities in pp collisions are predicted using the relation

$$\langle n'(s) \rangle_{pp} = \int_0^1 dK \chi(K, s) \langle n(K\sqrt{s}) \rangle_{e^+e^-}. \quad (4.4)$$

The parametrization (3.2) gives

$$\langle n'(s) \rangle_{pp} = 2.20s^{1/4} \langle K^{1/2} \rangle. \quad (4.5)$$

Equation (4.5) shows that the pure power-law growth of $\langle n'(s) \rangle$ of the $s^{1/4}$ type, which is good at low energies but too strong at collider energies, has slowed down because of the decreasing factor $\langle K^{1/2} \rangle$.

Two other parametrizations of $\langle n(W) \rangle_{e^+e^-}$, often used in the literature [17], are

$$(i) \quad \langle n(W) \rangle_{e^+e^-} = a + b \ln W^2 + c \ln^2 W^2, \quad (4.6)$$

$$a = 3.320, \quad b = -0.408, \quad c = 0.263,$$

and

$$(ii) \quad \langle n(W) \rangle_{e^+e^-} = a + b \exp c [\ln(W/Q_0)^2]^{1/2}, \quad (4.7)$$

$$a = 2.527, \quad b = 0.094, \quad c = 1.775, \quad Q_0 = 1 \text{ GeV}.$$

According to (4.4), these parametrizations yield

$$(i) \quad \langle n'(s) \rangle_{pp} = a_p + b_p \ln s + c_p \ln^2 s,$$

with

$$a_p = a + 2b \langle \ln K \rangle + 4c \langle \ln^2 K \rangle, \quad (4.8)$$

$$b_p = b + 4c \langle \ln K \rangle,$$

$$c_p = c,$$

and

$$(ii) \quad \langle n'(s) \rangle_{pp} \approx a + b \langle K^\alpha \rangle \exp[c (\ln(s/Q_0^2))^{1/2}],$$

with

$$\alpha = c / [\ln(s/Q_0^2)]^{1/2}, \quad Q_0^2 = 1 \text{ GeV}^2. \quad (4.9)$$

Here we have used

$$\langle \ln K \rangle = \psi(a) - \psi(a+b),$$

$$\langle \ln^2 K \rangle = \psi'(a) - \psi'(a+b) + \langle \ln K \rangle^2, \quad (4.10)$$

$$\langle K^\alpha \rangle = \frac{\Gamma(a+\alpha)}{\Gamma(a)} \frac{\Gamma(a+b)}{\Gamma(a+b+\alpha)},$$

where

$$\psi(x) = \frac{\Gamma'(x)}{\Gamma(x)} = \frac{d}{dx} \ln \Gamma(x).$$

All three parametrizations of $\langle n(W) \rangle_{e^+e^-}$ predict $\langle n'(s) \rangle_{pp}$, which is in reasonable agreement with the data (Table II).

The normalized moments $C'_q(pp)$. The energy variation of the normalized $C'_q = \langle n'_q \rangle / \langle n' \rangle^q$ moments in pp collisions is obtained from

$$C'_q(pp) = C_q(e^+e^-) \int dK \chi(K, s) \left[\frac{\langle n(K\sqrt{s}) \rangle_{e^+e^-}}{\langle n'(s) \rangle_{pp}} \right]^q. \quad (4.11)$$

This expression simplifies considerably if the power-law parametrization (3.2) of $\langle n(W) \rangle_{e^+e^-}$ is used:

$$C'_q(pp) = C_q(e^+e^-) \langle K^{q/2} \rangle / \langle K^{1/2} \rangle^q. \quad (4.12)$$

We can also calculate the dispersion

$$D^2(s)_{pp} = D'^2(s)_{pp} = \langle n^2(s) \rangle_{pp} - \langle n(s) \rangle_{pp}^2$$

of the multiplicity distribution in pp collisions. The result is

$$D(s)_{pp} = [C'_2(pp) - 1]^{1/2} \langle n'(s) \rangle_{pp}. \quad (4.13)$$

The average transverse momentum $\langle p_t(s) \rangle_{pp}$. The energy dependence of the average transverse momentum in pp collisions is obtained from

$$\langle p_t(s) \rangle_{pp} = \int_0^1 dk \chi(K, s) \langle p_t(K\sqrt{s}) \rangle_{e^+e^-}.$$

Using Eq. (3.5) we find that

$$\langle p_t(s) \rangle_{pp} = \alpha \langle K \rangle s^{1/2} + \beta. \quad (4.14)$$

The height of the central plateau $h(s)_{pp}$. The rise of the central plateau with energy in pp collisions is predicted from (3.6) to be

$$h(s)_{pp} = \langle h(K\sqrt{s}) \rangle_{e^+e^-}$$

$$= h_0 + h_1 \langle \ln K \rangle + \frac{1}{2} h_1 \ln s. \quad (4.15)$$

The forward-backward correlation strength $b(s)_{pp}$. From (3.9) we find that the forward-backward joint multiplicity distribution in pp collisions is of the form

$$P(n_F, n_B, s)_{pp} = P_n(s)_{pp} f_n(\Delta), \quad (4.16)$$

where $P_n(s)_{pp}$ is now given by (4.1).

The correlation strength $b(s)_{pp}$ is then

$$b(s)_{pp} = \frac{D^2(s)_{pp} - k \langle n'(s) \rangle_{pp}}{D^2(s)_{pp} - k \langle n'(s) \rangle_{pp}} \quad (4.17)$$

Using Eq. (4.13) and $k \approx 2$, we obtain

$$b(s)_{pp} = \frac{\langle n'(s) \rangle_{pp} [C'_2(pp) - 1] - 2}{\langle n'(s) \rangle_{pp} [C'_2(pp) - 1] + 2} \quad (4.18)$$

V. COMPARISON WITH DATA

In this section we compare predictions of Sec. IV with the available data on pp collisions. In order to obtain reasonable agreement with data, the inelasticity $\langle K \rangle$ should decrease with increasing incoming energy [24,26].

In this respect we follow the simple idea of Ref. [26] that the limited growth of the number of independently emitted sources $\langle C \rangle$ (clusters, clans, fireballs, . . .) is related to the decrease of $\langle K \rangle$ with energy in a very simple way:

$$\langle C(s) \rangle \sim \langle K(s) \rangle \ln s \quad (5.1)$$

We assume that $\langle K(s) \rangle \sim 4.1/\ln s$. Since there are no direct measurements of inelasticity except at ISR energies, the estimates of the actual rate of decrease of $\langle K(s) \rangle$ with energy may vary within the range of $\pm 20\%$. To be more specific, we use the set of parameters given in Table I to shape the $\chi(K,s)$ distributions (2.7), as shown in Fig. 1. Note that the parameters a and b vary with energy as [23]

$$a \sim 20/\ln s, \quad a + b \sim 5 \quad (5.2)$$

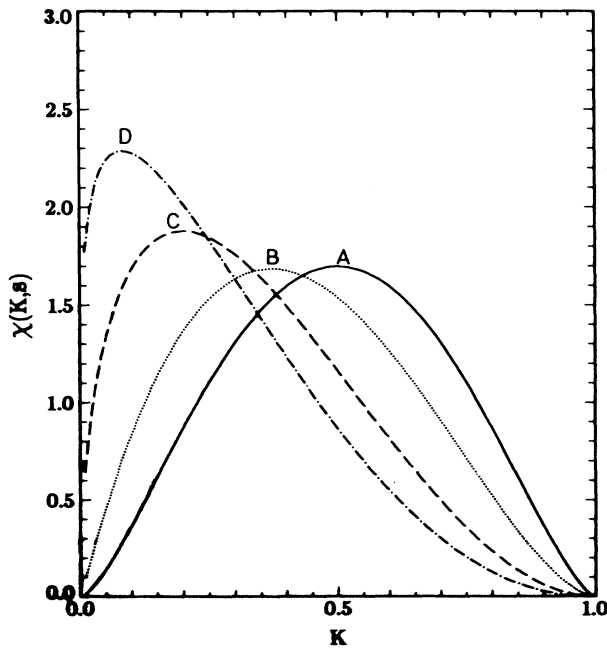


FIG. 1. The function $\chi(K,s)$ defined by Eq. (2.7) at various energies \sqrt{s} ($A = 16.5-63$ GeV, $B = 200$ GeV, $C = 540$ GeV, $D = 900$ GeV).

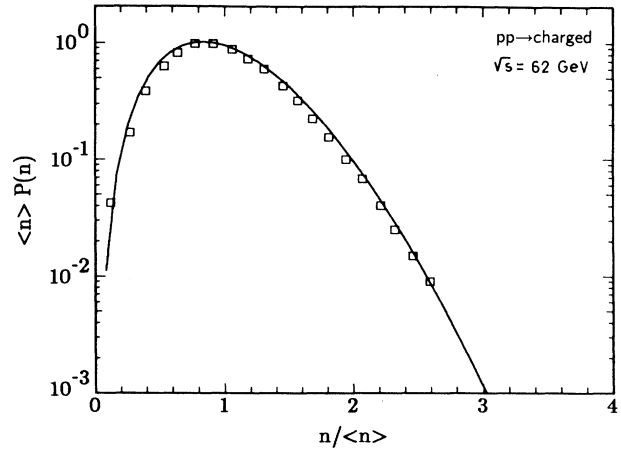


FIG. 2. Multiplicity distribution of charged hadrons in pp collisions at $\sqrt{s} = 62$ GeV in the KNO form. The data (\square) are from Ref. [37]. The theoretical curve (solid line) is from Eq. (4.1) of the text.

The predicted multiplicity distribution of charged hadrons in pp collisions at $\sqrt{s} = 62$ GeV in the KNO form is shown in Fig. 2 together with the data from Ref. [37].

According to Eq. (4.1) and Table I, the slope of the multiplicity distribution decreases with energy, roughly speaking, in proportion:

$$\langle K^{1/2} \rangle_{\sqrt{s}=900 \text{ GeV}}^2 : \langle K^{1/2} \rangle_{\sqrt{s}=540 \text{ GeV}}^2 : \langle K^{1/2} \rangle_{\sqrt{s}=200 \text{ GeV}}^2 \\ = 0.23 : 0.30 : 0.39 \quad (5.3)$$

This means that with increasing energy, the multiplicity distributions become wider than those predicted by the KNO scaling in the region of large z' .

It is interesting to note that a flat K distribution, $\chi(K,s) = 1$, $a = b = 1$, leads to the result obtained by Barshay [6] in deriving the KNO scaling in pp collisions from the e^+e^- data. The result is

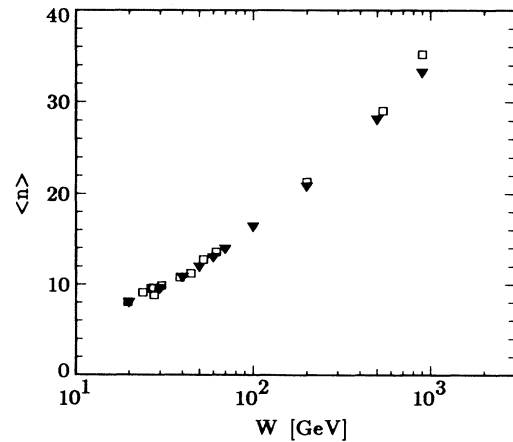


FIG. 3. Mean charged multiplicity in pp collisions. The data (\square) are from Ref. [14]. Our predictions (\blacktriangledown) follow from Eqs. (4.2) and (4.3) of the text.

TABLE I. Energy dependence of inelasticity.

\sqrt{s} (GeV)	a	b	$\langle K \rangle$	$\langle K^{1/2} \rangle$	$\langle \ln K \rangle$	$\langle \ln^2 K \rangle$
ISR	2.5	2.5	0.50	0.69	-0.80	0.91
200	2	2.7	0.42	0.63	-1.01	1.44
540	1.5	3	0.33	0.55	-1.35	2.51
900	1.2	3.2	0.27	0.48	-1.65	3.74
1800	1.1	3.3	0.25	0.46	-1.78	4.39
10^4	1.0	3.4	0.23	0.43	-1.94	5.17

$$\begin{aligned} \langle n'(s) \rangle_{pp} P_n(s)_{pp} &= \psi_{pp}(z') \\ &= (\pi/2) z' \exp[-(\pi/4) z'^2], \end{aligned} \quad (5.4)$$

with

$$z' = n / \langle n'(s) \rangle_{pp}.$$

Other predictions are compared with data in Figs. 3 and 4 and Tables II, III, and IV: in Fig. 3 and Table II for the average multiplicity, in Table III for the normalized moments and the dispersion, in Fig. 4 for the energy dependence of the mean transverse momentum, and in Table IV for the height of the central plateau and the strength of forward-backward multiplicity correlations. The agreement with the data is reasonable except for C'_q moments, which are clearly below the experimental data, in particular for higher moments. This is partly due to taking $n' = n - 2$. Better agreement is obtained if $n' = n - n_0$ with $n_0 < 1$, but still higher moments are not reproduced. Predictions for the Fermilab Tevatron collider energy ($\sqrt{s} \sim 1800$ GeV) and the extrapolation to the cosmic-ray point ($\sqrt{s} \sim 10^4$ GeV) are also given.

Breakstone *et al.* [37] analyzed the data on pp and $p\bar{p}$ multiplicities using the cuts at low (n_{\min}) and high (n_{\max}) multiplicities. We have calculated multiplicities using the same cuts. The results are given in Table V. Again, the agreement with the data [37] is reasonable.

VI. CONCLUDING REMARKS

Our analysis has shown that multihadron-production spectra in pp collisions can be quantitatively predicted from the corresponding e^+e^- annihilation data if a suitable averaging over the inelasticity distribution $\chi(K, s)$ is performed.

For a satisfactory account of the data, the $\chi(K, s)$

TABLE II. Predictions for the average charged multiplicity $\langle n'(s) \rangle_{pp}$.

\sqrt{s} (GeV)	$\langle n'(s) \rangle_{pp}$			
	Eq. (4.5)	Eq. (4.8)	Eq. (4.9)	Expt ^a
200	19.6	19.2	20.9	19.4
540	28.1	25.8	30.6	27.1
900	31.7	28.1	35.2	32.6
1800	42.9	34.2	46.7	
10^4	95.6	54.5	93.5	

^aSee Ref. [34] and note that $n' = n - 2$.

should depend on s in such a way that $\langle K \rangle$ decreases with increasing s [18].

The agreement between our predictions (Figs. 2, 3, and 4 and Tables II, III, IV, and V) and pp collision data seems to support the basic ansatz, Eq. (2.5), which relates the e^+e^- multiplicity distributions over a range of energies given by $W = K\sqrt{s}$ to the hadron multiplicity distribution at the given energy \sqrt{s} . However, the discrepancies are observed in C'_q moments for $q \geq 4$ and in the prediction of the rise of the rapidity plateau. These seem to indicate that for energies $\sqrt{s} > 100$ GeV not all aspects of pp collisions can be treated as an incoherent superposition of e^+e^- -like processes through Eq. (2.5).

It is necessary to stress here that our analysis is restricted to small- p_T hadron final states and to the two-jet structure similarity between e^+e^- and pp collisions.

We believe that the microscopic picture underlying Eq. (2.5) is that of Ref. [18]. The gluonic systems of the two incoming protons interact strongly and fragment subsequently in a manner similar to that for quark-antiquark pairs produced in e^+e^- annihilation. This obviously simple picture requires further study as it is not easy to see which QCD diagrams, if any, are responsible for the observed similarity between the hadronic spectra in e^+e^- and pp collisions.

There are also some simplified assumptions introduced into our calculations, such as the specific parametrization of $\chi(K, s)$ by the β function, and the particular KNO scaling form for e^+e^- multiplicity distributions [16].

Other input quantities concerning e^+e^- annihilation are basically experimental and may change in future experiments.

TABLE III. Predictions for the normalized moments according to Eq. (4.12). The corresponding experimental values [34] are given in parentheses, where $n' = n - 2$.

\sqrt{s} (GeV)	C'_2	C'_3	C'_4	C'_5	$\langle n' \rangle / D$
ISR	1.2	1.6	2.4	4.1	
200	1.20	1.71	2.73	4.84	2.18
	(1.31)	(2.12)	(3.92)	(8.51)	(1.78)
540	1.26	1.89	3.25	6.26	1.96
	(1.35)	(2.30)	(4.72)	(10.69)	(1.66)
900	1.31	2.10	3.84	8.02	1.79
	(1.38)	(2.38)	(4.83)	(10.94)	(1.61)
1800	1.33	2.18	4.17	9.01	1.74
10^4	1.40	2.36	4.73	10.73	1.58

TABLE IV. Predictions for the height of the central plateau $h_{pp}(s)$ and the strength of the forward-backward multiplicity correlations $b_{pp}(s)$.

\sqrt{s} (GeV)	$h_{pp}(s)^{a,b}$	$b_{pp}(s)^d$
200	4.39 ^c	0.32
540	4.44 ^c	0.57
900	4.73 ^c	0.66
1800	5.29	0.75
10 ⁴	6.04	0.90

^aExpt. data, Ref. [35].

^bExpt. data, Ref. [38].

^cA large part of the $p\bar{p}$ data is presented as $1/\sigma (d\sigma/d\eta)$, ($\eta=0$), where η is the pseudorapidity. To account for the change $\eta \rightarrow y$, the pseudorapidity data should be corrected [8,39] for comparison with our results. In the central region, $d\sigma/dy$ typically exceeds $d\sigma/d\eta$ by 10 to 20 %.

^dExpt. data, Refs. [32,36].

However, there are also additional important tests of the validity of Eq. (2.5), which have not been considered in the present paper.

This is the multiplicity dependence of $\langle p_t(s) \rangle$ in pp collisions and in e^+e^- annihilation where no data have been available up to now [9].

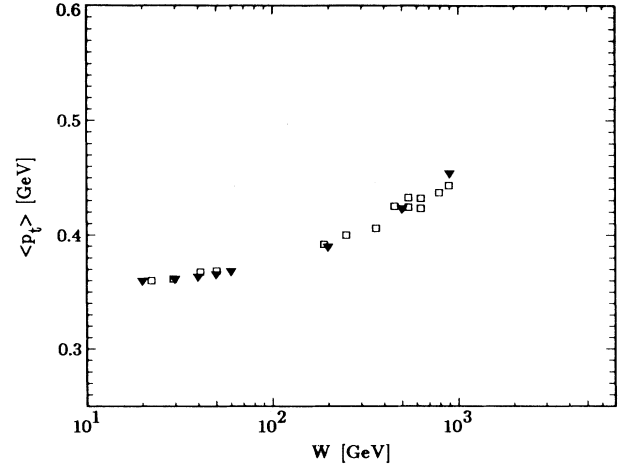


FIG. 4. Energy dependence of the mean transverse momentum in pp and $p\bar{p}$ collisions. The data (\square) are from Refs. [14,37]. Our predictions (\blacktriangledown) are obtained from Eq. (4.14) of the text.

The inclusion of hard processes when $\sqrt{s} > 100$ GeV has also not been discussed in this paper. We suggest a procedure similar to the geometrical model [40] and assume splitting of $\chi(K,s)$ in two parts:

TABLE V. pp and $p\bar{p}$ charged multiplicity distributions at different energies. The fits concern multiplicities n between the n_{\min} and n_{\max} values quoted in the table.

	\sqrt{s} (GeV)	n_{\min}	n_{\max}	$\langle n \rangle_{\text{NB}}^a$	$\langle n \rangle^b$
pp	10.7	4	14	5.57±0.14	5.87
pp	11.5	4	16	5.80±0.20	6.01
pp	13.8	4	18	6.51±0.18	
pp	13.8	4	18	6.51±0.20	
pp	13.8	4	18	5.99±0.35	6.41
$p\bar{p}$	13.8	4	18	6.65±0.10	
pp	13.9	4	18	6.33±0.15	6.42
pp	18.2	4	20	7.73±0.29	7.1
pp	19.7	6	22	7.98±0.17	8.45
pp	23.9	6	24	8.90±0.15	
					8.94
pp	23.9	6	24	9.07±0.24	
pp	26.6	6	24	9.40±0.14	9.25
pp	27.4	6	26	9.73±0.18	9.34
pp	27.6	6	26	9.36±0.17	
					9.36
pp	27.6	6	24	8.91±0.25	
pp	30.4	6	26	9.92±0.28	9.67
pp	38.8	6	32	10.64±0.11	10.55
pp	44.5	6	30	11.29±0.22	11.11
pp	52.6	8	34	12.68±0.24	12.87
pp	62.2	8	36	13.63±0.29	13.62
$p\bar{p}$	200	10	56	21.04±0.30	19.66
$p\bar{p}$	540	12	76	28.65±0.25	30.03
$p\bar{p}$	900	12	92	34.80±0.42	37.27

^aSee Table II of Ref. [37] and references therein.

^bThis paper.

$$\chi(K, s) = \chi_s(K) \theta(\sqrt{s} - \sqrt{s_0}) + \chi_h(K, s) \theta(\sqrt{s_0} - \sqrt{s}),$$

$$\sqrt{s_0} \sim 100 \text{ GeV},$$

where χ_s is due to soft collisions and χ_h is due to hard collisions.

The recent interest in multiplicity fluctuations related to intermittency may also be used to shed some light on the validity of Eq. (2.5). The problem here is the knowledge of the energy dependence of the intermittency index $f_q(W)$ for e^+e^- annihilation.

We hope to address these additional topics elsewhere.

-
- [1] M. Basile *et al.*, Phys. Lett. **92B**, 367 (1980); **95B**, 311 (1980); M. Basile *et al.*, Nuovo Cimento A **58**, 193 (1980).
- [2] D. Brick *et al.*, Phys. Lett. **103B**, 242 (1981).
- [3] F. Palmonari, lecture given at the Europhysics Study Conference on Jet Structure from Quark and Lepton Interactions, Erice, Sicily, 1982 [CERN Report No. CERN-EP/82-176, 1982 (unpublished)].
- [4] F. Takagi, Z. Phys. C **13**, 301 (1982).
- [5] C. B. Chiu and Qu-bing Xie, Phys. Rev. D **26**, 3057 (1982).
- [6] S. Barshay, Phys. Lett. **116B**, 193 (1982).
- [7] J. F. Gunion and G. Bertsch, Phys. Rev. D **25**, 746 (1982).
- [8] J. Kalinowski, M. Krawczyk, and S. Pokorski, Z. Phys. C **15**, 281 (1982).
- [9] M. Srczekowski and G. Wilk, Phys. Rev. D **44**, 577 (1991).
- [10] B. Anderson, G. Gustafson, and B. Nilsson-Almqvist, Nucl. Phys. **B281**, 289 (1987).
- [11] Z. Koba, H. B. Nielsen, and P. Olesen, Nucl. Phys. **B40**, 317 (1972).
- [12] W. Thome *et al.*, Nucl. Phys. **B129**, 365 (1977).
- [13] UA5 Collaboration, G. J. Alner *et al.*, Phys. Lett. **160B**, 199 (1985).
- [14] G. Giacomelli, Int. J. Mod. Phys. A **5**, 223 (1990).
- [15] Ch. Berger *et al.*, Phys. Lett. **95B**, 313 (1980).
- [16] TASSO Collaboration, M. Athoff *et al.*, Z. Phys. C **22**, 307 (1984); TASSO Collaboration, W. Braunschweig *et al.*, *ibid.* **45**, 193 (1989).
- [17] DELPHI Collaboration, P. Abreu *et al.*, Phys. Lett. B **247**, 137 (1990); Z. Phys. C **50**, 185 (1991).
- [18] G. N. Fowler, E. M. Friedlander, M. Plümer, and R. M. Weiner, Phys. Lett. **145B**, 407 (1984).
- [19] G. N. Fowler, R. M. Weiner, and G. Wilk, Phys. Rev. Lett. **55**, 173 (1985); G. N. Fowler, A. Vourdes, M. Weiner, and G. Wilk, Phys. Rev. D **35**, 870 (1987).
- [20] D. Brick *et al.*, Phys. Rev. D **25**, 2794 (1982).
- [21] M. Basile *et al.*, Nuovo Cimento A **73**, 329 (1983).
- [22] J. Wdowczyk and A. W. Wolfendale, Nature **306**, 347 (1983); Nuovo Cimento A **54**, 433 (1979); J. Phys. G **10**, 257 (1984); **13**, 411 (1987); E. M. Friedlander and R. M. Weiner, Phys. Rev. D **28**, 2903 (1983).
- [23] Y. T. Chou and C. N. Yang, Phys. Rev. D **32**, 1692 (1985); K. Watanabe and S. Tone, *ibid.* **39**, 195 (1989); R. C. Hwa and Ji-Can Pan, *ibid.* **45**, 106 (1992); M. T. Nazirov and P. A. Usik, J. Phys. G **18**, L7 (1992); I. Golyak, Mod. Phys. Lett. A **7**, 2401 (1992).
- [24] Yu. M. Shabelski, R. M. Weiner, G. Wilk, and Z. Włodarczyk, J. Phys. G **18**, 1 (1992).
- [25] J. Dias de Deus, Phys. Rev. D **32**, 2334 (1985); S. Barshay and Y. Ciba, Phys. Lett. **167B**, 449 (1986); T. K. Gaisser, in *Elastic and Diffractive Scatterings*, Proceedings, Evanston, Illinois, 1989, edited by M. M. Block and A. R. White [Nucl. Phys. B (Proc. Suppl.) **12**, 172 (1990)]; T. K. Gaisser, T. Stanev, S. Tilav, and L. Voyvodic, in *Proceedings of the Twenty-First International Cosmic Ray Conference*, Adelaide, Australia, 1989, edited by R. Protheroe (Graphic Services, Northfield, South Australia, 1990), Vol. 8, p. 55; J. N. Capdevielle, J. Phys. G **15**, 909 (1989); T. K. Gaisser and T. Stanev, Phys. Lett. B **219**, 375 (1989); B. Z. Kopeliovich, N. N. Nikolaev, and I. K. Potachnikova, Phys. Rev. D **39**, 769 (1989); J. Bellandi Fo, R. J. M. Covolan, C. Dobrigkeit, C. G. S. Costa, L. M. Mundim, and J. Dias de Deus, Phys. Lett. B **262**, 102 (1991); J. Bellandi, L. M. Mundim, J. Dias de Deus, and R. M. J. Covolan, J. Phys. G **18**, 579 (1992).
- [26] R. M. Weiner, G. Wilk, and Z. Włodarczyk, Phys. Rev. D **45**, 2308 (1992).
- [27] S. Barshay and Y. Yamaguchi, Phys. Lett. **51B**, 376 (1974).
- [28] P. Carruthers and M. Duong-Van, Phys. Rev. D **28**, 130 (1983).
- [29] S. Rudaz and P. Valin, Phys. Rev. D **34**, 2025 (1986).
- [30] N. Duinker, Rev. Mod. Phys. **54**, 356 (1982).
- [31] T. T. Chou and Cheu Ning Yaug, Phys. Lett. **135B**, 175 (1984); Phys. Rev. Lett. **55**, 1359 (1985).
- [32] UA5 Collaboration, K. Alpgård *et al.*, Phys. Lett. **123B**, 361 (1983).
- [33] *Handbook of Mathematical Functions*, edited by M. Abramowitz and I. A. Stegun (Dover, New York, 1965).
- [34] UA5 Collaboration, G. J. Alner *et al.*, Phys. Lett. **167B**, 476 (1986).
- [35] UA5 Collaboration, G. J. Alner *et al.*, Phys. Rep. **154**, 247 (1987); Z. Phys. C **33**, 1 (1987).
- [36] UA5 Collaboration, R. E. Ansorge *et al.*, Z. Phys. C **37**, 191 (1988).
- [37] A. Breakstone *et al.*, Nuovo Cimento A **102**, 1199 (1989).
- [38] CDF Collaboration, F. Abe *et al.*, Phys. Rev. D **41**, 2330 (1990).
- [39] C-Y. Wong, Phys. Rev. D **32**, 94 (1985).
- [40] R. C. Hwa, Phys. Rev. D **37**, 1830 (1989).